Revista Mexicana de Astronomía y Astrofísica, **49**, 351–356 (2013)

ATOMIC INTERPRETATION OF THE 13 KEV EMISSION FEATURE IN THREE AXPS: 4U 0142+61, XTE J1810-197 AND 1E 1048.1-5937

N. Koning, D. Leahy, and R. Ouyed

Department of Physics and Astronomy, University of Calgary, Calgary, Canada

Received 2013 June 4; accepted 2013 August 14

RESUMEN

En la última década, tres pulsores con emisión anómala en rayos X (AXPs) han mostrado una emisión en 13 keV en algunos de sus espectros. Este rasgo se interpreta comúnmente como debido a emisión protón-ciclotrón. Sin embargo, esta interpretación presenta varios problemas, incluyendo la coincidencia en 13 keV en las tres fuentes (lo cual implica el mismo campo magnético para las tres). En este trabajo investigamos la posibilidad de que la línea sea de origen atómico, así como las implicaciones que esto tendría para el entorno de los pulsores AXP.

ABSTRACT

In the past decade, three anomalous X-ray pulsars (AXPs) have shown emission features at ∼13 keV in some of their burst spectra. This feature is commonly interpreted as proton-cyclotron in nature. However there are several problems with this interpretation, including the coincidence at ∼13 keV in all three sources (implying the same magnetic field). In this paper we investigate the possibility that the line is atomic in origin, and the implications that this has for the environment around Anomalous X-Ray Pulsars.

Key Words: stars: individual (XTE J1810-197, 4U 0142+61, 1E 1048.1-5937) — stars: magnetic field — stars: neutron

1. INTRODUCTION

Anomalous X-Ray Pulsars (AXPs) are solitary objects characterized by persistent emission, X-ray pulsations and a rapid spin down rate. These objects generally exhibit spin periods of 5–12 seconds, X-ray luminosities in the range of $\sim 1 \times 10^{33}$ erg s^{-1} to $\sim 1 \times 10^{36}$ erg s^{-1}, soft X-ray spectra, and rapid spin down rates of $\dot{P} = 1 \times 10^{-13} \rightarrow 1 \times 10^{-10}$ s s^{-1} (Woods et al. 2005). AXPs can go through major flux variation during rare, Soft Gamma-ray Repeater (SGR) – like X-ray bursts. The first detected AXP was 1E 2259-586 (Fahlman & Gregory 1981) and since then, several more have been discovered including 1E 1048.1-5937, 4U 0142+61, 1E 1547.0-5408, 1RXS J170849.0-400910, 1E 1841-045, XTE J1810-197, CXOU J010043.1-721134, and CXO J164710.2-455216. AXPs and SGRs share many properties, and are thought to be related phenomena.

The leading model to explain the AXP phenomenon is the magnetar model (Thompson & Duncan 1995). Magnetars are neutron stars (NS) with extreme magnetic fields between $\sim 1 \times 10^{14}$ and $\sim 1 \times 10^{15}$ G. The bursting mechanism in the magnetar model may be located on the NS surface, or in the magnetosphere. In one model the large magnetic field exerts stress on the crust, causing it to fracture and subsequently emit short X-ray bursts. These "starquakes" are believed to create additional hotspots on the surface of the NS (Pons & Rea 2012). Another model suggests that reconnection events of a highly twisted magnetic field create the bursts in the magnetosphere (Lyutikov, Thompson, & Kulkarni 2002). The spin-down rate and periods observed in AXPs are explained through a combination of magnetic-breaking and magnetic field decay on a time-scale shorter than the spin-down time-scale. The magnetar model has been developed over the past 15 years and has been highly successful in explaining many properties of AXPs and SGRs. Other models have been put forth to explain properties of AXPs, including the Fall-Back Disk model (Chat-

terjee, Hernquist, & Narayan 2000) and the Quark Nova model (Ouyed, Leahy, & Niebergal 2007a,b).

During the quiescent phases, AXP spectra below ∼10 keV are often featureless with a continuum characterized by the sum of a power law and a black body, the sum of two black bodies or even by resonant cyclotron scattering (Rea et al. 2008). Emission lines have been observed in the spectra of three AXPs during their bursting phase; 4U 0142+61 (Gavriil, Dib, & Kaspi 2011), XTE J1810-197(Woods et al. 2005) and 1E 1048.1-5937 (Gavriil, Kaspi, & Woods 2006)[1].

In the magnetar model, the line is commonly interpreted as a cyclotron line, implying field strengths $\sim 2.2\times10^{15}$ G for protons and $\sim 1.2\times10^{12}$ G for electrons (Gavriil, Dib, & Kaspi 2008). The cyclotron interpretation does have some challenges: if due to protons, the inferred magnetic field ($\sim 2.2\times10^{15}$ G) is much larger than that derived by magnetic breaking ($\sim 1.3 - 3.3 \times 10^{14}$ G). This can be reconciled with non-dipolar fields however, because the spin down rate depends on the dipolar component, whereas the line gives the field at the surface. If the line is an electron cyclotron line, the implied field is too low for the surface of the magnetar, and thus requires emission from far above the surface (∼100 km due to the nature of a dipole field). Another complication is that there are other significant lines detected (at ∼8 keV in 4U 0142+61). If these are also proton cyclotron lines, then the emission must be coming from multiple, distinct regions on the magnetar surface, possibly providing evidence for a multipolar field. Finally, as noted by e.g., Gavriil et al. (2011), it is very unlikely that all three AXPs have features at similar energies when their inferred magnetic fields differ by a factor of 3.

In this paper we consider the possibility that these emission features are atomic in origin. If this is the case, the identification of the responsible transition has the potential to provide crucial information about the bursting environment.

2. OBSERVATIONS

Gavriil, Kaspi, & Woods (2002) was the first to report an emission line in the spectra of Burst 1 from the 2001 outburst of 1E 1048.1-5937. They were able to best fit the spectrum with a one-component power-law and a Gaussian emission line at 14.2 ± 1.1 keV. Woods et al. (2005) observed an emission line in the spectra of Burst 4 from XTE J1810-197. They were able to best fit the spectrum with a black body (3.6 keV) plus a Gaussian emission line at 12.6 ± 0.2 keV. Gavriil et al. (2006) reported the detection of another emission line in the spectra of 1E 1048.1-5937, this time from Burst 3 of the 2004 event. For this burst, they were able to best fit the spectrum with a Gaussian emission line at 13.09 ± 0.25 keV and a black body at ∼3 keV. Because the error in this measurement is much smaller than that from Burst 1 of the 2001 event, we will use this result in our line analysis. Finally, Gavriil et al. (2011) reported an emission feature at ∼13 keV in Burst 6 of 4U 0142+61. Their best fit model included a Gaussian emission line at 14.2 ± 0.3 keV and a black body at 5.8 keV. The spectra of each source is given in Figure 1 and a summary of the best fit Gaussian energy is presented in Table 1 for reference[2].

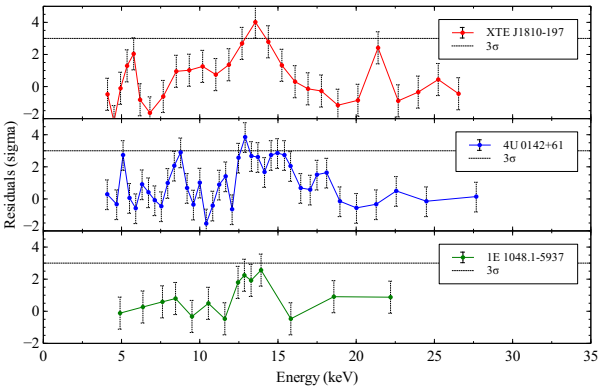

Fig. 1. Observed emission line spectrum from three different AXP sources: XTE J1810-197, 4U 0142+61 and 1E 1048.1-5937 (Burst 3). These spectra represent the residuals after subtraction of the best fit continuum. All show a strong, significant feature at ∼13 keV. Data from Gavriil et al. (2011). The color figure can be viewed online.

3. RESULTS

In this analysis, we assume that the emission feature seen in each AXP is caused by the same, single, atomic transition. The discrepancy between line energies (see Table 1) therefore allows us to gain insight into some physical and geometric conditions of each system.

We will investigate three scenarios which may lead to the observed features:

[1] In the case of 1E 1048.1-5937, a significant feature has been observed in two of the three bursts (Gavriil et al. 2006, 2002)

[2] In our analysis we use the Gaussian line centers quoted above (the best fits according to the discovery papers). We do not attempt to independently fit the spectrum of each source ourselves.

TABLE 1

OBSERVED CHARACTERISTICS OF THE AXPS IN THIS STUDY INCLUDING THE BEST FIT GAUSSIAN LINE CENTER FOR THE 13 KEV FEATURE

AXP	Line Center (keV)	P (s)	dP/dt (s/s)	τ (years)
4U 0142+61	14.2 ± 0.3 (Burst 6)	8.69	0.203×10^{-11}	68000
XTE J1810-197	12.6 ± 0.2 (Burst 4)	5.54	0.777×10^{-11}	11000
1E1048.1-5937	13.09 ± 0.25 (Burst 3)	6.46	2.25×10^{-11}	4500

Data for P, dP/dt and characteristic age, obtained from McGill Pulsar Group at `http://www.physics.mcgill.ca/ pulsar/magnetar/main.html`.

1. The emission is from a disk in Keplerian orbit around the NS.
2. The emission is from a static or co-rotating region around the NS.
3. The emission is from the surface of the NS.

3.1. *Scenario I*

The first scenario involves emission from a Keplerian disk in orbit around the NS. For this analysis we will assume the NS has a mass of 1.5 $M_\odot$ and a radius of 10 km. For a Keplerian orbit, we have the constraint $\beta = v/c = \sqrt{GM/rc^2}$ where r is the radius of the disk.

There are two primary ways in which the location of the observed line may differ from that emitted: gravitational red-shift and Doppler shift. The Doppler shift is a combination of radial and transverse, where transverse always results in a red-shift. In a disk geometry, the radial Doppler shift yields a split line, with a red and blue components. If the disk is relativistic, the blue component will be more intense than the red one, due to relativistic beaming (see, e.g, Fabian et al. 1989). It is fair to assume therefore that if the emission feature in our AXPs is from a relativistic disk, we would detect the blue-side of the split line.

Quantitatively, the shift in energy of the line from an emitted energy of E_e to an observed energy of E_o, $\Delta = E_e - E_o$, is a combination of:

$$\Delta_{\rm grav} = E_e \left(1 - \sqrt{1 - 2\beta^2}\right) , \quad (1)$$

$$\Delta_{\rm trans} = E_e \left(1 - \sqrt{1 - \beta^2}\right) , \quad (2)$$

$$\Delta_{\rm rad} = E_e \left(1 - \sqrt{\frac{1 + |\beta| \sin(\theta)}{1 - |\beta| \sin(\theta)}}\right) , \quad (3)$$

where θ is the inclination of the disk. We have used the absolute value of β in equation 3 because we are only interested in the blue (negative velocity) component. The observed line peak is therefore a combination of each shift:

$$E_o = E_e - (\Delta_{\rm grav} + \Delta_{\rm trans} + \Delta_{\rm rad}) . \quad (4)$$

We use equation 4 to calculate the radius of the disk at different inclinations for each AXP source. As examples, we use energies of $E_e = 14.7$ keV (Sr XXXVII, strongest transition in the NIST[3] database in our range) and $E_e = 12.0$ keV. We chose these two values in order to show an example on either side of the 13 keV line (a net red-shift and a net blue-shift). The results are displayed in Figure 2. We notice that for a given E_e only a certain range of disk inclinations ($\theta_0 - \theta_1$) are possible (either there is no possible way to shift E_e to E_o, or the location of the disk lies below the surface of the NS).

We can calculate the probability that each disk inclination is within this range:

$$\mathrm{Prob}(\theta_0, \theta_1) = |\cos(\theta_1) - \cos(\theta_0)| ,$$

and by multiplying each together determine the likelihood that all three AXPs have Keplerian disks inclined within their respective ranges. For $E_e = 14.7$ keV, we get $\mathrm{Prob_{4U}} = \mathrm{Prob}(0, 37) = 0.20$, $\mathrm{Prob_{J18}} = \mathrm{Prob}(0, 25.5) = 0.1$, $\mathrm{Prob_{1E}} = \mathrm{Prob}(0, 29) = 0.13$, giving a combined probability of Prob = 0.0026. For $E_e = 12.0$ keV, $\mathrm{Prob_{4U}} = \mathrm{Prob}(62, 90) = 0.47$, $\mathrm{Prob_{J18}} = \mathrm{Prob}(46, 90) = 0.69$, $\mathrm{Prob_{1E}} = \mathrm{Prob}(50.5, 90) = 0.63$, giving a combined probability of Prob = 0.20. We perform this same probability calculation for all energies between 10 and 20 keV (in intervals of $dE = 0.01$ keV) and plot the results in Figure 3 (blue line). The line energy that gives the highest probability of each AXP having an allowed disk inclination is at $E_e \sim 12.5$ keV with Prob ~ 0.3. There is no atomic line at this

[3]National Institute of Standards and Technology, `http://www.nist.gov/`.

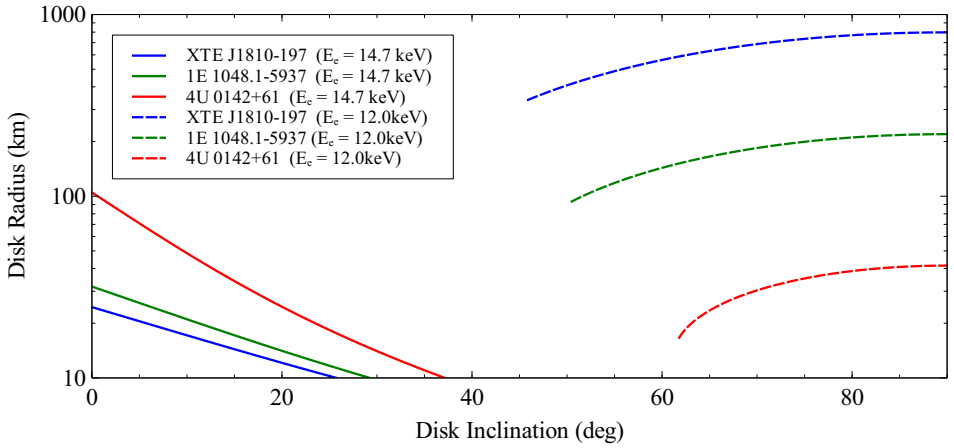

Fig. 2. Keplerian disk radius versus inclination for each AXP source using equation 4. In each case the NS has a mass of 1.5 $M_\odot$ and a radius of 10 km. Two different possible line energies are considered, E_e at 14.7 keV and E_e at 12 keV. For any given E_e only a certain range of inclinations are possible. The color figure can be viewed online.

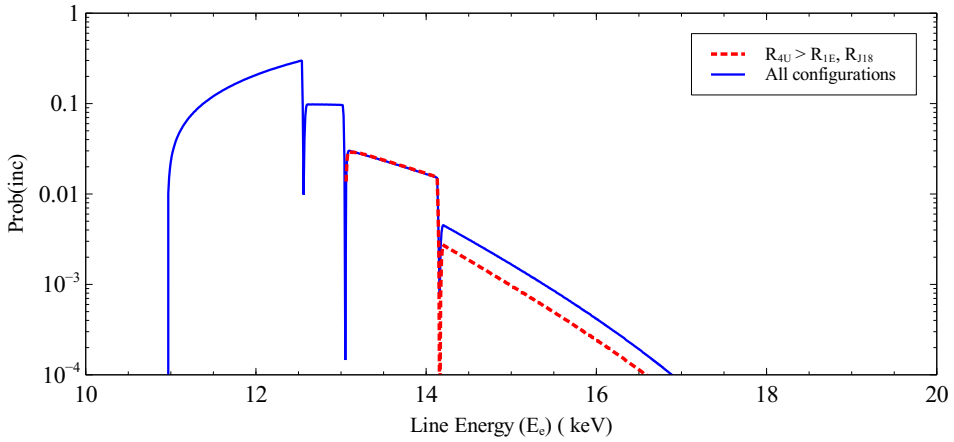

Fig. 3. Plot of the probability that all systems are at an allowed inclination versus energy of the emitted line (E_e). The blue solid line represents all possible configurations, whereas the red dotted line represents only those configurations where the radius of 4U 0142+61 is greater than the other two. The highest probability in all configurations case is at $E_e = 12.5$ keV and for the restricted case, at $E_e = 13.1$ keV. The color figure can be viewed online.

TABLE 2

ALLOWED KEPLERIAN DISK RADIUS (SCENARIO I) AND LOCATION OF EMISSION REGION (SCENARIO II) FOR EACH AXP[a]

	Scenario I		Scenario II	
AXP	$R_{\rm min}$ (km)	$R_{\rm max}$ (km)	$R_{\rm min}$ (km)	$R_{\rm max}$ (km)
4U 0142+61	10.0	9.9×10^4	15.2	∞
XTE J1810-197	10.0	95.3	10.0	20.8
1E1048.1-5937	10.0	187.3	11.1	29.5

[a]Assuming a NS with mass 1.5 $M_\odot$ and radius 10 km.

energy in the NIST database, the closest being Ga XXXI at 12.7 keV.

To progress in this analysis we have to make some further assumptions. If the disk spreads due to viscous forces, and each system is born with a disk of similar radius, we expect the older systems to have the larger disks. The characteristic age (τ) of an AXP can be determined from its period (P) and period derivative (dP/dt):

$$\tau = \frac{P}{2dP/dt}\,. \tag{5}$$

Table 1 gives the characteristic age of each AXP, with that of 4U 0142+61 much larger than the other two. We therefore assume that 4U 0142+61 has the largest disk. The red, dashed line in Figure 3 is the probability that each system is in an allowed inclination and that the disk radius of 4U 0142+61 is the largest. In this case the line energies are restricted between ≈13 keV $\leq E_e \leq$ ≈16.5 keV, with the highest probabilities occurring between ≈13 keV $\leq E_e \leq$ ≈14 keV. Lines from the NIST database within this range include Kr XXXV, Kr XXXIV and Rb XXXVI. The allowed disk radii for line energies between 13 and 16.5 keV is given in Table 2.

3.2. *Scenario II*

The second scenario involves emission from a static or co-rotating structure. Again we will assume the NS has a mass of 1.5 $M_\odot$ and a radius of 10 km. If the emission region is slowly rotating, the Doppler shift is negligible and only the gravitational red-shift can be responsible for the different peak energies in each AXP. We can immediately reach several conclusions about the energy, E_e, of the atomic transition.

Since we only have a red-shift, and the highest energy line is that of 4U 0142+61 at 14.2 keV, we require that $E_e \geq 14.2$ keV. Furthermore, the largest gravitational red-shift would occur on the surface of the NS (10 km). The energy of a line emitted from the surface of the NS whose observed energy is E_o is given by:

$$E_e = \frac{E_o}{\sqrt{1 - 2GM/c^2 r}}\,. \tag{6}$$

The lowest energy line is that of J1810-197 at $E_o = 12.6$ keV, allowing us to conclude that $E_e \leq$ 16.88 keV.

Knowing the energy of the emitted line allows us to calculate the radius of the emission region:

$$r = \frac{2GM}{c^2}\left(\frac{E_e^2}{E_e^2 - E_o^2}\right)\,. \tag{7}$$

We calculate the minimum and maximum radius using the observed energies (E_o) from Table 1 and the range for E_e given above. The results are presented in Table 2.

3.3. *Scenario III*

Our final scenario assumes that the emission of the line comes from the surface of the NS. The difference in energy of the observed features is therefore due solely to gravitational red-shift. As in Scenario II, this requires $E_e \geq 14.2$ keV.

Equation 6 suggests that the least amount of gravitational red-shift occurs when the ratio M/r is smallest. From Figure 3 in Steiner, Lattimer, & Brown (2013), the smallest M/r ratio allowed under current theoretical models for a compact object is 0.3 $M_\odot$/15 km. Using equation 6 with this value, we get $E_e \geq 14.64$ keV. Again from Figure 3 in Steiner et al. (2013), $M/r < 2.5$ $M_\odot$/11 km, giving $E_e \leq 22.0$ keV. Therefore, if the emission originates from the surface of the NS, the transition responsible lies between 14.64 keV $\leq E_e \leq$ 22 keV.

4. CONCLUSION AND DISCUSSION

We have examined the implications on the line energy and emission region around each AXP in three different scenarios. The first scenario considers a Keplerian disk around a NS. We found that only specific inclinations are possible for each line energy, E_e, and used that result to calculate the probability of finding each AXP disk at an allowed inclination. This yielded a range of possible energies for the line, from ∼11 keV to ∼17 keV, with the most probable at ∼12.5 keV. If we assume that the oldest system (4U 0142+61) has the largest disk, we can restrict the range of possible line energies further to ≈13 keV $\leq E_e \leq$≈16.5 keV. Furthermore, only certain disk radii are possible for each system, allowing us to restrict the disk location.

The second scenario examined the possibility that the line is emitted from a static or co-rotating region around the NS. Under this scenario we conclude that the line must be emitted between $E_e =$ 14.20 and 16.88 keV. Using this range of energies, we calculated the possible radii of the emission regions to be 15.2 km $\leq r < \infty$ for 4U 0142+61, 10.0 km $\leq r \leq$ 20.8 km for XTE J1810-197 and 11.1 km $\leq r \leq$ 29.5 km for 1E 1048.1-5937.

In the last scenario we looked at emission from the surface of the NS. Using theoretical models constraining the M/r ratio of compact objects, we conclude that the transition must lie between 14.64 and 22 keV.

It is difficult to determine the species responsible for the emission feature. The intensity depends on the density and temperature of the species, and the transition probability of the line. Although the strongest line reported in the NIST database between 10 and 20 keV is Sr XXXVII at 14.669 keV, we know very little of the density or temperature of the emitting region. Perhaps there is no Sr, or the temperature is too low to excite the transition. One clue as to the temperature comes from the black body fits performed for each source. In all cases, the black body temperature was $\geq$3 keV (3.5×10^7 K). In order to see a line in emission, the emission region must be hotter than the background, implying a temperature $\geq$3 keV. It is interesting to note that the ionization energy of Sr XXXVI (giving Sr XXXVII) is $\sim$4.6 keV (5.3×10^7 K) (Sansonetti 2011), which makes the SrXXXVII transition at 14.669 keV plausible. Our probability analysis for the first scenario suggests that the energy leading to the highest probability that each system is in an allowed inclination is $\sim$12.5 keV. However there is no atomic transition at this energy, and no strong transitions are in the vicinity (according to the NIST database). Although other transitions are possible within the allowed energies, there is no a-priori reason for us to assume one species exists and the others do not. Under this reasoning, the strongest line within the allowed range, SrXXXVII, is our most likely candidate.

Despite the limited information we have, we have been able to constrain the possible energies of the transition. If we assume that older systems have larger disks, then the line energy must be between $\sim$13 and 22 keV. Although we cannot pinpoint the exact energy, it is interesting to note that the strong Sr XXXVII line does lie within this range. Furthermore, almost all transitions above 13 keV are due to r-process elements, which may provide important constraints for AXP models.

Future observations of AXP sources showing emission features at $\sim$13 keV will further constrain the transition and nature of the emission region. In the case of a Keplerian disk, a less intense red component of the line should exist. If this is observed in the future, it will pinpoint the line energy and confirm the Keplerian disk hypothesis. Once the transition is determined, we can use it to probe the density and temperature of the emission region providing important insights into the nature of AXPs.

This work is funded by the Natural Sciences and Engineering Research Council of Canada. N.K. would like to acknowledge support from the Killam Trusts.

REFERENCES

Chatterjee, P., Hernquist, L., & Narayan, R. 2000, ApJ, 534, 373
Fabian, A. C., Rees, M. J., Stella, L., & White, N. E. 1989, MNRAS, 238, 729-736
Fahlman, G. G., & Gregory, P. C. 1981, Nature, 293, 202
Gavriil, F. P., Dib, R., & Kaspi, V. M. 2008, in AIP Conf. Proc. 983, 40 Years of Pulsars: Millisecond Pulsars, Magnetars and More, ed. C. G. Bassa, Z. Wang, A. Cumming, & V. M. Kaspi (New York: AIP), 234
_____. 2011, ApJ, 736, 138
Gavriil, F. P., Kaspi, V. M., & Woods, P. M. 2002, Nature, 419, 142
_____. 2006, ApJ, 641, 418
Lyutikov, M., Thompson, C., & Kulkarni, S. R. 2002, in ASP Conf. Ser. 271, Neutron Stars in Supernova Remnants, ed. P. O. Slane, & B. M. Gaensler (San Francisco: ASP), 262
Ouyed, R., Leahy, D., & Niebergal, B. 2007a, A&A, 473, 357
_____. 2007b, A&A, 475, 63
Pons, J. A., & Rea, N. 2012, ApJ, 750, L6
Rea, N., Zane, S., Turolla, R., Lyutikov, M., & Goumltz, D. 2008, ApJ, 686, 1245
Sansonetti, J. E. 2011, J. Phys. Chem. Ref. Data, 41, 013102
Steiner, A., Lattimer, J., & Brown, E. 2013, ApJ, 765, L5
Thompson, C., & Duncan, R. C. 1995, MNRAS, 275, 255
Woods, P. M., et al. 2005, ApJ, 629, 985

N. Koning, D. Leahy, and R. Ouyed: Department of Physics and Astronomy, University of Calgary, Calgary, AB, T2N 1N4, Canada (nico.koning, leahy, rouyed@ucalgary.ca).